Sci.Int.(Lahore),28(4),4241-4247,2016 ISSN 1013-5316;CODEN: SINTE 8

DIAGNOSTIC SIMULATION OF SINGLE PHASE INDUCTION MOTOR NOISE WITH DIFFERENT PWM SCHEMES

Nabeel Khalid[1], Umar Tabrez Shami[2], Arslan Ashraf[3], Adeel Arif[4]

[1,3,4] University of Central Punjab, Lahore, Pakistan

[2] University of Engineering and Technology, Lahore, Pakistan

[1]nabeel.khalid@ucp.edu.pk, [2]ushami@ymail.com, [3]arslan.ashraf@gmail.com, [4]adeel.arif@ucp.edu.pk

ABSTRACT—*The single phase induction motor (SPIM) is observed to generate noise whenever fed by inverter. The noise generated by the motor depends on the harmonics in the current. Operation of single phase induction motor when fed by an inverter is investigated by simulating four PWM schemes i.e. sine-wave PWM, third harmonic injected PWM, trapezoidal PWM and triangular PWM. The scope of the work includes the simulation of single phase induction motor model and selection of PWM scheme with least harmonics. Flux and current of the stator is analyzed with the aid of the above-mentioned schemes. It is shown that the simulated model produces the desired results and the motor produces less current and flux harmonics for Trapezoidal PWM and most current and flux harmonics for third harmonic injected PWM.*

Index Terms—AC Motor, AC Motor Drive, PWM Schemes Selection, Acoustic noise

I. INTRODUCTION

Single phase induction motor when driven by a non-sinusoidal current i.e. through an inverter that has the current with many time harmonics that leads to noise generation. The noise created by an induction motor has an impingement on the surroundings. Many research papers show various reasons regarding the generation of noise includes the structure of motor, space harmonics of motors, current supplied to the stator, etc. [1,2,3].

In induction motors, the noise is thus generated by different sources. The ventilating system produces a noise which is more in case of small motors as compared to large size motors because the speed of fan increases as number of poles decreases [1]. Heating of bearings causes the mechanical noise which is structural hazard and it has very low significance [1]. The electromagnetic source of noise is of greater interest for this research being the dominant source of noise in machines with more number of poles. More number of poles makes the height of stator yoke smaller due to which it deforms easily [1]. The deformation of stator is due to the time harmonics present in the current supplied to the motor which affects the flux developed in the air gap. [2]. The ventilating system noise lies in the range of 500 to 1000 Hz, while the bearing noise has a frequency range of 3 kHz and more [4]. The electromagnetic noise has a frequency range of 500 Hz to 3.5 kHz [5]. The frequency spectrum of the three sources lie in the audible spectrum which is from 20 Hz to 20 kHz.

When motor is driven by current with harmonics, some flux rich in harmonics is the result. This flux causes the magnetic stress in the air gap present. The effect of this stress deforms the stator yoke. This deformation of stator results in the radiation of noise from the motor. The effect of magnetic forces on the rotor is very small due to slip in induction motors. Due to slip, the frequency of the rotor magnetic field is very small. The decrease in the rotor frequency decreases the effect of magnetic stress on the rotor [6].

Noise can be reduced by improving the design of the motor, i.e., by selecting proper number of stator and rotor slots, choosing low flux density in air gap, balancing of rotor, etc. [1]. The noise reduction is also possible by reducing radial force density waves through the injection of current harmonics with low amplitudes. This injection of current harmonics counters the force density waves present in the air gap for the harmonics except the fundamental. [7]. The noise can be reduced by employing an active or passive filter. The filtration technique helps to eliminate the unwanted frequencies in the flux spectrum or by filtering only the required frequency in the spectrum [8]. The low switching PWM and slope PWM techniques can be used as one of the solutions [9] [10].

This paper focuses on the comparison of motor behavior when induction motor is driven by an inverter. Four different PWM schemes including sine PWM, Third Harmonic Injected PWM, Trapezoidal PWM, and Triangular PWM for the inverter are considered to develop a correlation between noise and harmonic content in the current flowing through the stator and flux developed on stator when driven by selected PWM scheme.

In this paper, section-1 presents the literature review and research work already done, section-2 describes the modeling of the single phase induction motor and the results obtained after simulation, section-3 discusses the four PWM schemes used to simulate the motor behavior. In section-4, the experimental results are presented. Section-5 discusses the conclusions based on the simulation results while section-6 contains the references.

II. INDUCTION MOTOR MODELLING

Single phase induction motor is an unsymmetrical machine. The function of the motor is based on two phase machine having two windings i.e. main and auxiliary winding. The parameters of auxiliary winding are mostly same as main winding but with an electrical displacement of 90^{o}. The main winding is considered as first phase while the auxiliary is considered as second phase of the machine [11].

DQ transformation may be used for modeling of motor. Based on this, main winding is represented as direct axis winding while the auxiliary winding as the quadrature winding. Based on dq transformation, following equivalent circuits are formed [12].

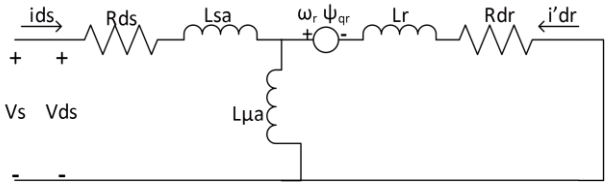

Figure-1 Equivalent circuit for Direct Axis Winding

4242 ISSN 1013-5316;CODEN: SINTE 8 Sci.Int.(Lahore),28(4),4241-4247,2016

This part will present the modelling of single phase induction motor. To model the induction motor, two windings will be considered, the quadrature winding and the direct axis winding. The modelling is performed by using the equivalent circuit of induction motor for quadrature and direct axis windings [12].

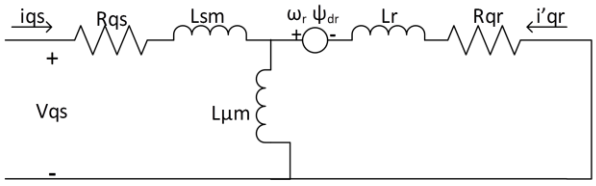

Figure-2 Equivalent Circuit for Quadrature axis Winding

The modeling of motor is performed by the following equations [13] derived from the two circuits above.

$$v_{qs} = \frac{d\psi_{qs}}{dt} + R_{qs} i_{qs} \quad (1)$$

$$v_{ds} = \frac{d\psi_{ds}}{dt} + R_{ds} i_{ds} \quad (2)$$

$$v_{qr} = \frac{d\psi_{qr}}{dt} + R_{qr} i_{qr} - \omega_r \psi_{dr} \quad (3)$$

$$v_{dr} = \frac{d\psi_{dr}}{dt} + R_{dr} i_{dr} - \omega_r \psi_{qr} \quad (4)$$

$$\psi_{qs} = L_{sm} i_{qs} + L_{\mu m}(i_{qs} + i_{qr}) \quad (5)$$

$$\psi_{ds} = L_{sa} i_{ds} + L_{\mu a}(i_{ds} + i_{dr}) \quad (6)$$

$$\psi_{qr} = L_r i_{qr} + L_{\mu m}(i_{qs} + i_{qr}) \quad (7)$$

$$\psi_{dr} = L_r i_{dr} + L_{\mu a}(i_{ds} + i_{dr}) \quad (8)$$

Where, ψqs, ψds, ψqr, ψdr are Flux linkage for quadrature and direct axis windings, Lsm, Lsa, Lμm, Lsa, are the self and mutual inductances for quadrature and direct axis windings, Lr is the Self inductances of rotor winding, ωr is the Speed of rotor, vqs, vqr, vds, vdr are Stator and Rotor voltages for quadrature and direct axis windings, and iqs, iqr, ids, idr are Stator and Rotor currents for direct and quadrature axis windings.

The instantaneous electromagnetic torque and speed of the rotor is represented as [12]:

$$T_e = p\left(\psi_{qr} i_{dr} - \psi_{dr} i_{qr}\right) \quad (9)$$

$$\omega_r = \frac{d\theta_r}{dt} \quad (10)$$

Where p is the number of poles, and θ_r is the angular displacement between stator and rotor.

These equations are used to model the induction motor. This model is implemented in MATLAB and analyzed for an induction motor of 150W, 220V, 2 poles, 50 HZ [13]. The torque speed curve of the motor is shown in figure-3.

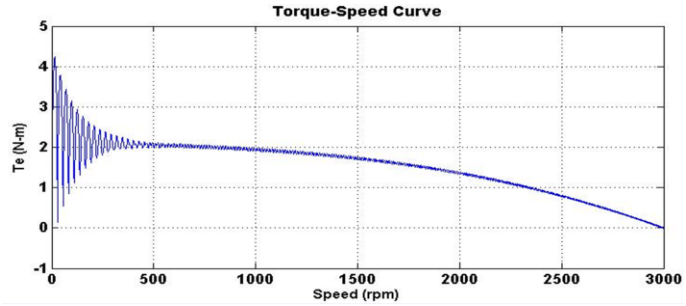

Figure-3 Torque-Speed characteristics

Simulated torque speed curve is compared against the result presented in [13]. The result is found to be the same as presented which justifies the correctness of model.

III. PWM SCHEMES

In this section, the generation of PWM schemes is discussed. The four schemes which are used include:

i. Sine Wave PWM
ii. Third Harmonic Injected PWM
iii. Trapezoidal Wave PWM
iv. Triangular Wave PWM

These PWM schemes are generated by the comparison of a high frequency switching signal with a low frequency signal. The amplitude of the generated PWM depends on the amplitude modulation index (m_a), while the presence of harmonics in the output depends on the frequency modulation index (m_f).

To generate the PWM that has an amplitude linearly varying with the switching signal, m_a should be from 0 to 1 that represents the linear modulation. If m_a is greater than 1, then over modulation is observed. In case of over modulation, the output contains many more harmonics in the side band than the linear mode of operation.

The selection of m_f is such that it should be an integer and preferably be an odd integer of fundamental frequency which results in the elimination of even harmonics. To have a synchronous PWM, m_f should be small. This results in the elimination of subharmonics [14].

Based on the above discussion, for the generation of the PWM schemes, m_f is chosen as 21 which is an odd multiple of the fundamental harmonic and upper limit of the range, while m_a is chosen as 0.9 to remain in the linear range of operation. The PWM schemes presented in figures 4 – 7 are obtained at the output of the inverter.

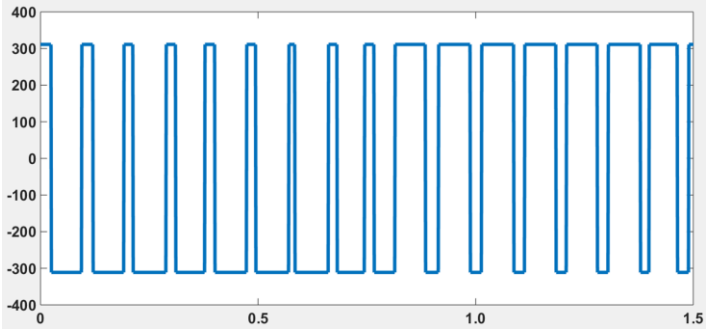

Figure-4 Sine Wave PWM

Sci.Int.(Lahore),28(4),4241-4247,2016 ISSN 1013-5316;CODEN: SINTE 8

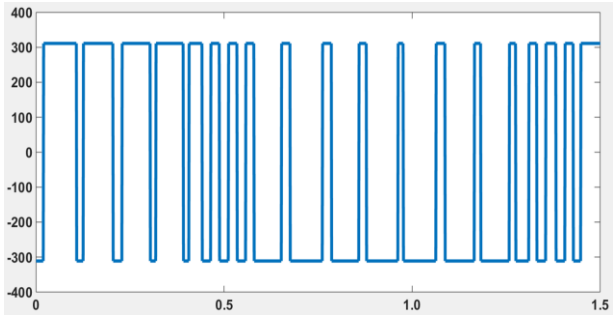

Figure-5 Third Harmonic Injected PWM

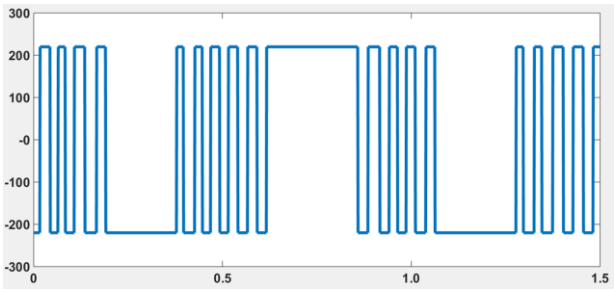

Figure-6 Trapezoidal PWM

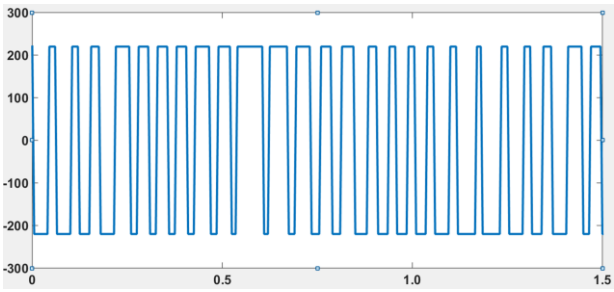

Figure-7 Triangular PWM

These PWM schemes are applied to the motor to evaluate the behavior of the motor.

IV. Simulation Results

The magnetic forces generate the magnetic stress in the air gap between stator and rotor. The magnetic stress is mathematically represented as [6]:

$$P_{mr} = 0.5.B_{m1}.B_{m2}.\cos[(\omega_1+\omega_2).t+(k+l).\alpha+(\phi_1+\phi_2)] \\ +0.5.B_{m1}.B_{m2}.\cos[(\omega_1+\omega_2).t+(k-l).\alpha+(\phi_1-\phi_2)] \quad (11)$$

Where, B_{m1} and B_{m2} are the flux densities of stator and rotor, ω_1 and ω_2 are the angular frequency of stator and rotor, k and l are the space harmonics of stator and rotor. The above equation shows the stress the air gap is directly dependent on the flux density of stator and rotor. Due to slip, the effect of harmonics will be very small on rotor as compared to stator. In this paper, the flux of stator is thus analyzed for the four PWM schemes mentioned earlier.

The experimental results are divided into two parts. First the currents flowing through the stator, its frequency response, flux developed on stator and its frequency response for each PWM scheme is discussed. While in the second part comparison of current magnitudes is presented.

A. Results of Different PWM Techniques

The results of four PWM techniques including sine PWM, Third Harmonic Injected PWM, Trapezoidal PWM, and Triangular PWM are shown. The results include the waveforms for current and flux, along with their respective frequency responses.

The flux in a closed magnetic path directly depends on the current flowing through the coil, mathematically represented as [15].

$$\phi = \frac{\mu NA}{l} I$$

$$\phi \alpha I$$

Where, μ is the permeability, N is the number of turns, A is the area of cross section of the core, l is the mean length of the core, ϕ is the flux through the core, and I is the current flowing through the coil.

This shows that any variation in current has a direct impact on the flux. This relationship of current and flux is represented in the following results.

Sine PWM

The current flowing through the stator and its frequency response is shown in figure 8 and 9. The flux developed on stator and its frequency response is shown in figure 10 and 11.

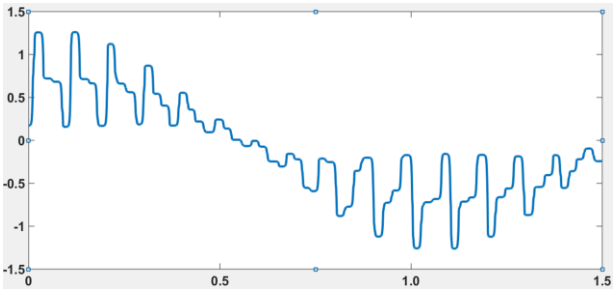

Figure-8 Stator Current for Sine PWM

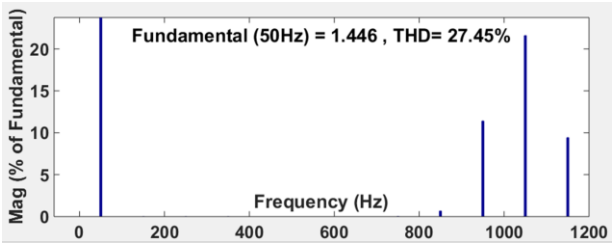

Figure-9 FFT of Sine Wave PWM Current

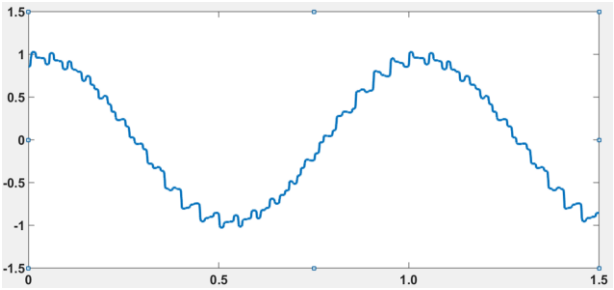

Figure-10 Stator Flux for Sine PWM

4244 ISSN 1013-5316;CODEN: SINTE 8 Sci.Int.(Lahore),28(4),4241-4247,2016

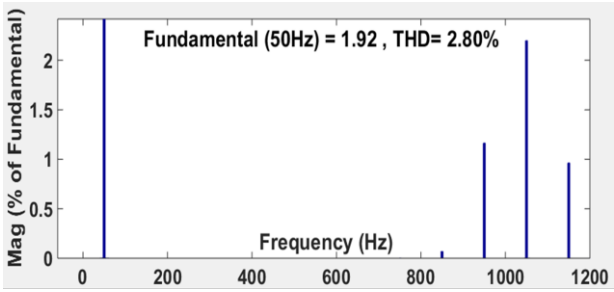

Figure-11 FFT of Stator Flux for Sine PWM

As can be seen in figure 9, the frequency response of current which contains only fundamental harmonic along with the switching harmonic only, while figure-11 shows the flux which also has the fundamental and side bands of switching harmonics. The variation in flux obeys the variation in current. The swells in the flux are present exactly at the same instant as the current as that of current shown in figures 8 and 10. The presence of only fundamental harmonic and the side bands of switching harmonics depicts the correctness of the model of the motor as discussed earlier. These are the expected responses when a motor is excited by a sine wave PWM.

Total harmonic distortion (THD) is the measure of harmonic content present in the current with respect to the fundamental harmonic. The THD for current is 27.45% while for flux is 2.8%. This THD value shows that the total amplitude of all the harmonics is 27.4% of the fundamental harmonic of the current while in case of flux it is 2.8% of the fundamental harmonic.

ii. Third Harmonic Injected PWM

The current flowing through the stator and its frequency response is shown in figure 12 and 13. The flux developed on stator and its frequency response is shown in figure 14 and 15.

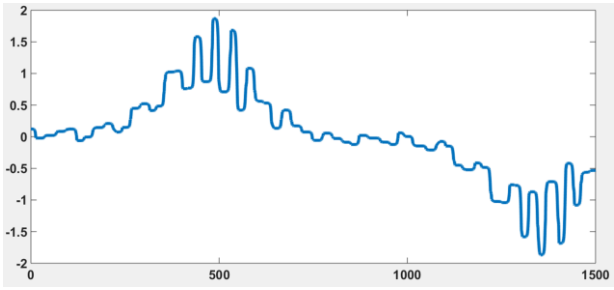

Figure-12 Stator Current for THI PWM

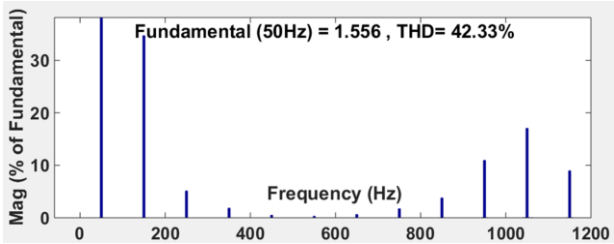

Figure-13 FFT of Stator Current for THI PWM

The injection of third harmonic increases the amplitude of voltage as compared to sinewave amplitude. The increase in voltage increases the current drawn by the motor.

In figure 13, we can see the frequency response of stator current, the presence of 3rd, 5th and 7th harmonics along with the switching harmonics makes the THD of 42.33%. This increase in THD depicts the increase in the harmonic content in the stator current. In fig-15 the frequency response for flux also shows the presence of 3rd, 5th and 7th harmonic along with switching harmonics. The THD value for flux is 4.78%. As the harmonic content is more than the sine wave PWM, so the THD value is also more than sine wave PWM.

The ripples present in the stator flux are on the same instants as of current as shown in figures 12 and 14, which shows the direct dependence of flux on current. The results shown by the motor model are as expected by the motor.

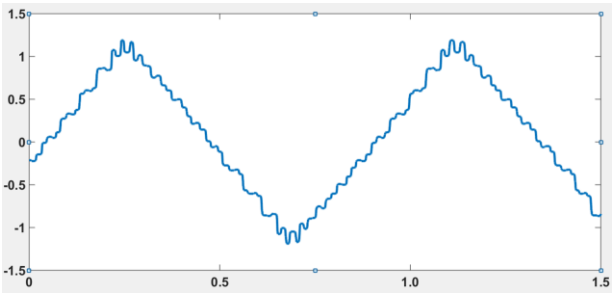

Figure-14 Stator Flux for THI PWM

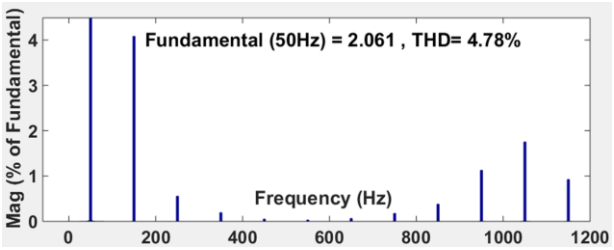

Figure-15 FFT of Stator Flux for THI PWM

iii. Trapezoidal PWM

The current flowing through the stator and its frequency response is shown in figure 16 and 17. The flux developed on stator and its frequency response is shown in figure 18 and 19.

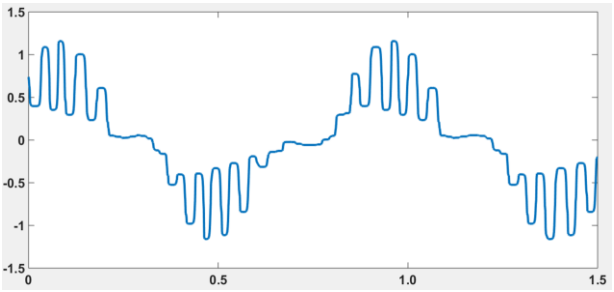

Figure-16 Stator Current for Trapezoidal PWM

Sci.Int.(Lahore),28(4),4241-4247,2016 ISSN 1013-5316;CODEN: SINTE 8

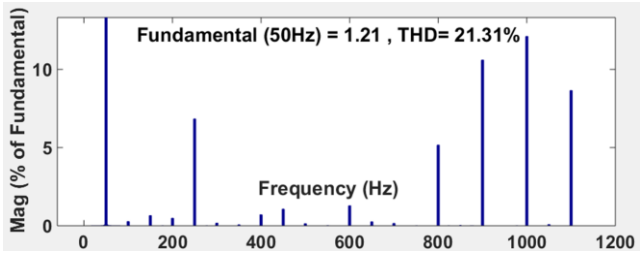

Figure-17 FFT of Stator Current for Trapezoidal PWM

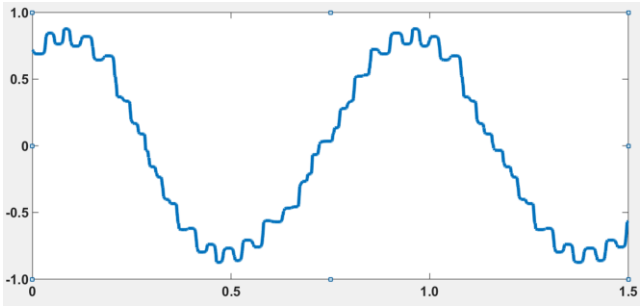

Figure-18 Stator Flux for Trapezoidal PWM

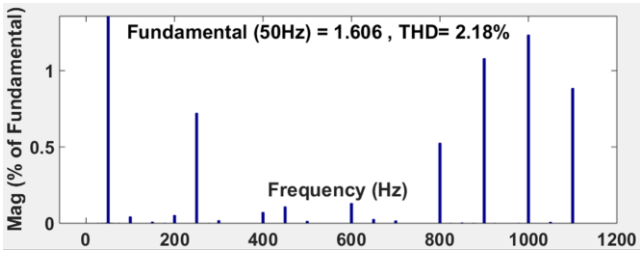

Figure-19 FFT of Stator Flux for Trapezoidal PWM

Frequency response of stator current is presented in figure 17, which contains multiple harmonics but with low amplitudes. The low amplitudes of harmonics other than fundamental makes the THD small and it is 21.32 % for current. In figure-19 the frequency response of flux also depicts the same frequency response as current. Just like the current THD for flux is 2.18%. The decrease in the THD value shows the decrease in the harmonic content as compared to sine PWM and THI PWM.

The distortion in the current and flux are less as compared to THI PWM. The flux ripples are on the same time instant as of current which shows the direct dependence of flux on current as depicted by figures 16 and 18. The results shown by the motor model are as expected by the motor.

iv. Triangular PWM

The current flowing through the stator and its frequency response is shown in figure 20 and 21. The flux developed on stator and its frequency response is shown in figure 22 and 22.

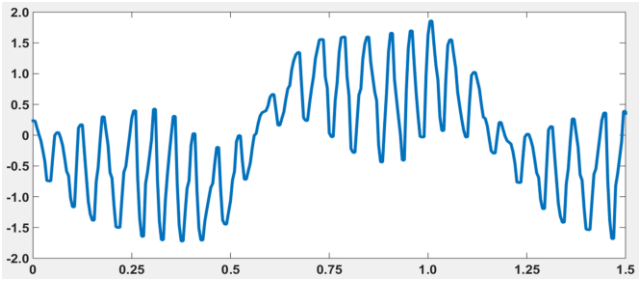

Figure-20 Stator Current for Triangular PWM

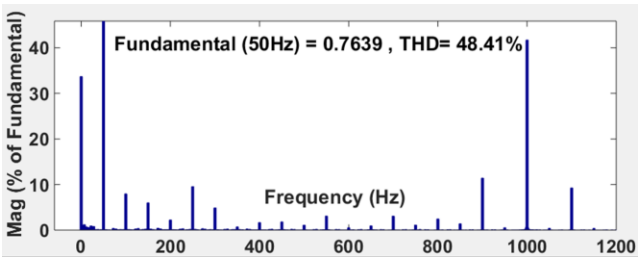

Figure-21 FFT of Stator Current for Triangular PWM

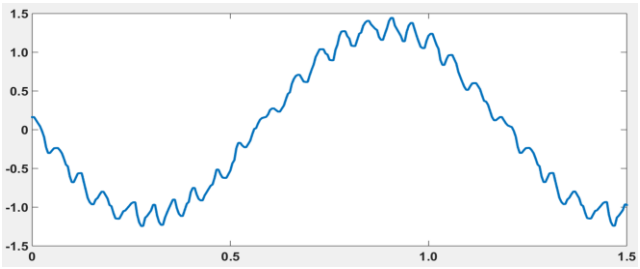

Figure-22 Stator Flux for Triangular PWM

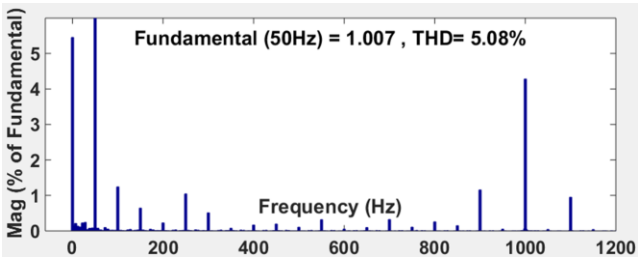

Figure-23 Stator Flux for Triangular PWM

We can see in figure-2, the frequency response of stator current has higher harmonics as well as the sub harmonics. The THD of current is 48.41% which shows more harmonic content with respect to fundamental harmonic. In figure-23 the frequency response of flux also has the same behavior as of current. The THD value for flux is 5.08%. This PWM current has the highest THD among the four PWM schemes, because the harmonics content is very high in this PWM scheme.

The current and flux in case of triangular PWM have the highest distortions. The results for current and flux show that there are so many combers present in the current and flux due to triangular wave PWM while the trapezoidal PWM has the least swells present.

The figures 20 and 22 show that the swells present in the current are transferred to the flux as the flux is directly proportional to the current. The results shown by the motor model are as expected by the motor.

B. Comparison of Current magnitudes

Presented below is the comparison of RMS value of current for four PWM schemes. Figure 24 shows the comparison of RMS values of current for four PWM schemes.

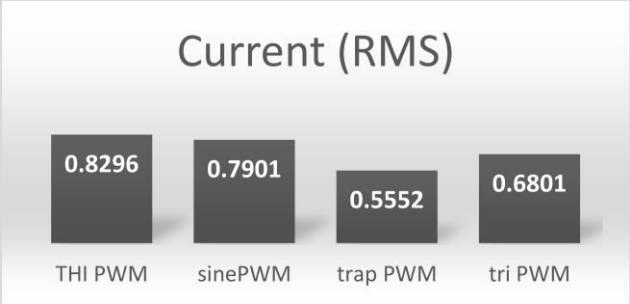

Figure-24 Current Magnitudes

As can be seen from the figure-24, the motor draws maximum current when supplied by the third harmonic injected PWM, while it draws minimum current when supplied by the trapezoidal PWM.

V. CONCLUSION

The modeling of single phase induction along with simulation of motor model with the aid of above mentioned PWM schemes has been presented taking into account the selection of PWM scheme with least harmonics. The proposed model produces the desired results. The PWM schemes satisfies the desired criteria. The simulation of motor with the aid of Sine Wave PWM depicts that the Total harmonic distortion (THD) for current is 27.45% while for the flux is 2.8%. When motor model is simulated with the aid of Third harmonic injected PWM, the THD is 42.33% for current and 4.78% for flux. The model simulation with Trapezoidal PWM shows that the THD for current is 21.31% and for flux is 2.18% and finally the simulation with Triangular PWM shows the current THD as 48.41% and flux THD as 5.08%. The comparison of current drawn by the motor for four PWM schemes is also presented. As discussed in section-IV, the noise depends on the stress in air gap. The stress depends on the flux density of the stator flux and rotor flux. The harmonics in the flux are maximum for Third Harmonic Injected PWM while minimum for Trapezoidal PWM. Based on all the results presented in the paper and the dependence of stress on the harmonics in flux, it is concluded that the noise will be maximum when driven by Third Harmonic Injected PWM while minimum when driven by Trapezoidal PWM.

VI REFERENCES

[1] S. L. Nau and H. G. G. Mello, "ACOUSTIC NOISE IN INDUCTION MOTORS: CAUSES AND SOLUTIONS," in *Petroleum and Chemical Industry Conference, 2000*, San Antonio, TX , 2000.

[2] Miyashita, B. K. Ichiro and S. Sone, "Novel Prediction Method of Acoustic Magnetic Noise," in *Power Conversion Conference*, Nagaoka, 1997.

[3] A. Negoita, A. N'diaye and A. Djerdir, "The magnetic noise of the inverter-fed permanent split-capacitor induction motor," in *Electrical Machines (ICEM)*, Marseille, 2012.

[4] C. Schlensok, B. Schmülling, M. v. Giet and K. Hameyer, "Electromagnetically excited audible noise Evaluation and optimisation of electrical machines by numerical simulation," *COMPEL: The International Journal for Computation and Mathematics in Electrical and Electronic Engineering*, vol. 26, no. 3, p. 727 – 742, 2007.

[5] J. F. Gieras, C. Wang and J. C. Lai, Noise of Polyphase Electric Motors, Taylor & Francis Group, LLC, 2006.

[6] M. Janda, O. Vitek and V. Hajek, "Noise of Induction Machines," in *Induction Motor Modeling and Control*, Brno University of Technology, Czech Republic, 2012.

[7] D. Franck, M. v. d. Giet and K. Hameyer, "Active reduction of audible noise exciting radial force-density waves in induction motors," in *IEEE International Electric Machines & Drives Conference (IEMDC)*, 2011.

[8] J. Ferreira, P. Dorland and F. d. Beer, "An Active In-Line Notch Filter for reducing Acoustic Noise in Drives," in *Industry Applications Conference*, 2004.

[9] A. Ruiz-Gonzalez, F. Vargas-Merino, F. Perez-Hidalgo, M. J. Meco-Gutierrez and J. Heredia-Larrubia, "Low switching PWM strategy to reduce acoustic noise radiated by inverter-fed induction motors," in *IEEE International Symposium on Industrial Electronics* , Bari, 2010.

[10] A. Ruiz-González, F. Vargas-Merino, J. R. Heredia-Larrubia, M. J. Meco-Gutiérrez and a. F. Pérez-Hidalgo, "Application of Slope PWM Strategies to Reduce Acoustic Noise Radiated by Inverter-Fed Induction Motors," *IEEE TRANSACTIONS ON INDUSTRIAL ELECTRONICS*, vol. 60, no. 7, pp. 2555-2563, July 2013.

[11] M. Prazenica, P. Sekerak, L. Kalamen and B. Dobrucky, "Two-phase power electronic drive with split Single-phase induction motor," in *IECON (36th Annual Conference on IEEE Industrial Electronics Society)*, Glendale, AZ , 2010.

Sci.Int.(Lahore),28(4),4241-4247,2016 ISSN 1013-5316;CODEN: SINTE 8

[12] S. Sarkar, S. Paul, S. Samaddar, S. Sarkar, P. K. Saha and G. K. Panda, "Modelling, Analysis and Simulation of Split Phase Type Single Phase Induction Motor," *International Journal of Advanced Research in Electrical, Electronics and Instrumentation Engineering*, vol. 2, no. 5, May 2013.

[13] V. Hrabovcova, L. Kalamen and P. S. a. P. Rafajdus, "Determination of Single Phase Induction Motor Parameters," in *International Symposium on Power Electronics, Electrical Drives, Automation and Motion*, 2010.

[14] N. Mohan, T. M. Undeland and W. P. Robbins, Power Electronics, John Wiley & Sons, INC..

[15] S. J. Chapman, Electric Machinary Fundaments, McGraw-Hill, 2005.

[16] D.-J. Kim, J.-W. Jung, J.-P. Hong, K.-J. Kim and C.-J. Park, "A Study on the Design Process of Noise Reduction in Induction Motors," *IEEE TRANSACTIONS ON MAGNETICS*, vol. 48, no. 11, pp. 4638-4641, November 2012.